Suppression of decomposition of aniline cation in intense laser fields by cluster formation with NH_3 and H_2O

Ryuji Itakura, Taiki Asano, Kaoru Yamanouchi*

Department of Chemistry, School of Science, The University of Tokyo, 7-3-1 Hongo, Bunkyo-ku, Tokyo 113-0033, Japan

Abstract

Using a tandem-type time-of-flight (TOF) mass spectrometer, the mass-selected aniline (AN)–water cluster cations, $[AN(H_2O)_n]^+$ ($n = 1, 2$), were irradiated with the intense femtosecond (fs) laser fields ($\lambda \sim 395$ nm, $I \sim 5 \times 10^{15}$ W/cm^2, $\Delta t \sim 50$ fs). By the cluster formation with H_2O, decomposition of AN^+, $AN^+ \rightarrow C_5H_6^+ + HNC$, induced by the intense fs laser fields was significantly suppressed. From the observation that the suppression of the decomposition of AN^+ occurs from $[AN(H_2O)_n]^+$ more efficiently than from $[AN(NH_3)_n]^+$ ($n = 1, 2$), the effect of the cluster formation on the decomposition process was discussed.
© 2003 Elsevier Science B.V. All rights reserved.

Keywords: Tandem mass spectrometer; Intense laser fields; Aniline cation; Aniline–ammonia cluster cation; Aniline–water cluster cation; Suppression of decomposition

1. Introduction

When diatomic and triatomic molecules are irradiated with intense laser fields whose magnitude is comparable with that of Coulomb fields within a molecule, multiple ionization proceeds in most cases, leading to the formation of multiply charged parent molecules. Such highly charged molecules are known to decompose instantaneously into charged atomic fragment ions with large kinetic energies, which is called Coulomb explosion [1–4]. Along with the expansion of the target molecules, it has been shown that the formation of the multiply charged molecules is not always a major process and that a resonance coupling between the electronic states of a parent molecule with a specific charge number could play a decisive role in the ionization and fragmentation processes especially for relatively large molecules [5–8]. It was found for a number of organic molecules with a π conjugation that the ionization into the doubly charged state was significantly suppressed and that the fragmentation at the singly charged state occurred dominantly when the wavelength of the laser light fields matches the energy gap between the electronic ground state and the electronically excited state in the singly charged state.

In our recent work on benzene [6] and aniline (AN) [8], the singly charged parent cations were irradiated selectively with intense laser fields using a tandem-type mass spectrometer. When the laser field wavelength (λ) was $\lambda \sim 395$ nm, the fragmentation occurred efficiently via the resonance coupling between the electronic ground and excited states of the singly charged cation stage.

Recently, we have revealed for an AN cation (AN^+) that the decomposition processes in intense laser fields are significantly suppressed by the cluster formation with NH_3 [8]. Because it is probable that the first and second NH_3 molecules are bound to the amino group of AN^+ through the hydrogen bonding, the suppression could be influenced by changing the character of the hydrogen bond by replacing NH_3 with other molecules.

In the present study, in order to investigate the mechanism of the suppression we prepare selectively singly charged $[AN(H_2O)_n]^+$ ($n = 1, 2$) with the tandem-type mass separation technique, and examine how their responses to the intense femtosecond (fs) laser fields ($I \sim 5 \times 10^{15}$ W/cm^2) are different from those of $[AN(NH_3)_n]^+$. Once the dependence of dynamical behavior of molecules in intense laser fields on such cluster formation is understood, it would become possible to design a photochemical reaction under the intense laser fields not only by synthesizing optimized laser fields but also by preparing an appropriate type of clusters.

* Corresponding author. Tel.: +81-3-5841-4334; fax: +81-3-5689-7347.
E-mail address: kaoru@chem.s.u-tokyo.ac.jp (K. Yamanouchi).

2. Experimental

The $AN(H_2O)_n$ clusters are formed under jet-cooled conditions by expanding the He buffer gas carrying AN and water vapors into a vacuum chamber through a pulsed valve at the stagnation pressure of around 0.5 atm. The gas mixture is prepared by flowing He gas bubbles through the AN–water mixture stored in the reservoir.

The $AN(H_2O)_n$ clusters are irradiated with the fourth harmonic ($\lambda = 266$ nm) of a Nd:YAG laser (GCR130, Spectra-Physics), and are ionized into $[AN(H_2O)_n]^+$ through a two-photon process. Using a tandem-type time-of-flight (TOF) mass spectrometer, they are mass-selected and exposed to intense laser fields in the same manner as described previously in our recent studies [6,8].

As shown schematically in Fig. 1, at the first stage of the tandem-type mass spectrometer, the parent ions are accelerated at ∼3.9 kV by Wiley–McLaren-type three parallel electrode-plates, and are temporally and spatially mass-separated after the flight through the 1 m length field-free region. In the central part of the field-free region a mass gate composed of a pair of parallel electrode plates is located along the TOF axis. As shown in the inset of Fig. 1, the pulsed high voltage is applied to the mass gate to deflect undesired ions whose signals might overlap the signals of the ions generated by irradiating the mass-selected cations with the intense laser fields at the second stage of the tandem-type mass spectrometer. The ion packet with a kinetic energy of ∼3.9 keV is decelerated in the region between the grounded entrance grid and the second grid with a voltage of 1.4 kV. When the mass-selected $[AN(H_2O)_n]^+$ ($n = 1, 2$) reaches the point equidistant from the second grid and the third grid, they are exposed to the intense laser fields generated by focusing the fs laser light ($\Delta t \sim 50$ fs,

$\lambda \sim 395$ nm). Finally, the product ions produced by the interaction of the mass-selected parent ions with the intense laser pulse are re-accelerated in the region between the third grid with a voltage of 1.5 kV and the exit-grid with a ground level potential. After drifting through the second 1 m length field-free region, the product ions are temporary mass-separated and detected by an MCP detector whose signals are sent to a digital oscilloscope (9384, Lecroy) with a 1 GHz sampling rate.

The fs laser system is composed of a mode-locked Ti–sapphire laser system (Millennia, Spectra-Physics and Mira-Seed, Coherent) and a regenerative amplifier system (Alpha10, B.M. Industries). The details of the fs laser system were described previously [6]. The fs laser pulses at $\lambda \sim 395$ nm of ∼1 mJ/pulse were obtained by frequency doubling of the amplified Ti–sapphire output by a β-BBO crystal (1 mm thick) after the pulse compression. The peak intensity of the fs laser fields generated by focusing the amplified pulses through a quartz lens ($f = 300$ mm) is estimated to be ∼5×10^{15} W/cm^2 at the focal point.

3. Results and discussion

3.1. $C_5H_6^+$ formation from AN^+, $[AN(NH_3)_n]^+$, and $[AN(H_2O)_n]^+$ ($n = 1, 2$) in intense laser fields

It was found as shown in Fig. 2 that the mass-selected AN^+ exposed to intense fs laser fields undergoes the fragmentation mainly into $C_5H_6^+$ without being ionized into the doubly charged cation [8]. When AN^+ with a C_{2v} planar structure is exposed to the 395 nm laser fields, a charge-resonant coupling between the ground $^2B_1$ and excited $^2B_1$ states could occur through the large transition
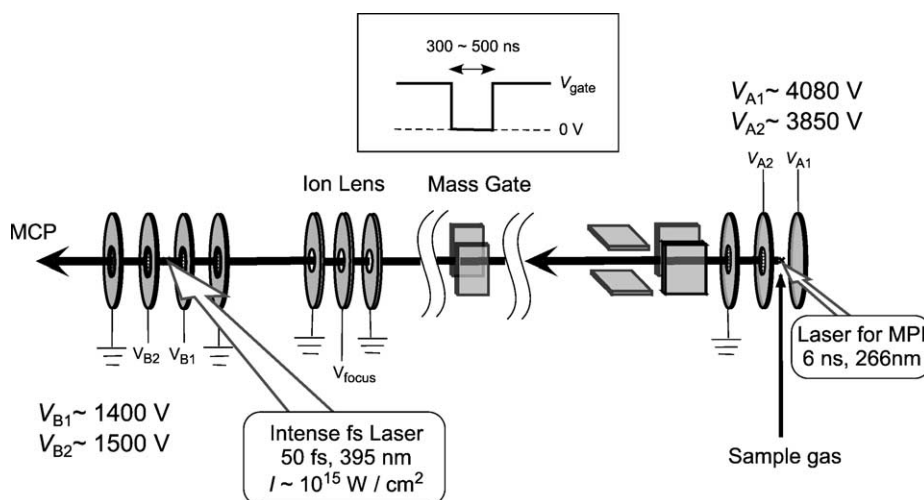

Fig. 1. The schematic diagram of the tandem-type TOF mass spectrometer. The first TOF stage is composed of three electrode grids and two pairs of deflectors. The inset shows the diagram of the pulsed high voltage applied to the mass gate to allow only the desired ions to pass through. In the second TOF stage the ions with specific mass and charge numbers are decelerated in the region between the first and second electrode grids and are exposed to the intense laser fields at the center of the second and third grids. The product ions are re-accelerated in the region between the third and fourth electrode grids.
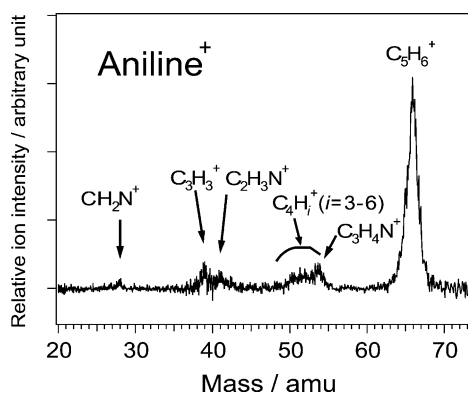
Fig. 2. The mass spectrum obtained when the mass-selected AN^+ ($C_6H_5NH_2^+$) was irradiated with the intense fs laser pulses ($\lambda \sim 395$ nm, $I \sim 5 \times 10^{15}$ W/cm^2) [8].

dipole moment [9–11], since the energy gap between these two states is close to the photon energy at $\lambda \sim 395$ nm. It is expected that the potential energy surfaces of the $^2B_1$ and $^2B_1$ states of AN^+ are deformed through the formation of the light-dressed states, and that the nuclear dynamics of AN^+ is governed by the temporary varying dressed-state potential energy surfaces. Through such a resonant coupling, a resonant stimulated-Raman process accompanied by an immediate internal conversion process could be induced, and eventually AN^+ would gain sufficiently large internal energy for the rapid decomposition into $C_5H_6^+$.

When one or two NH_3 molecules are attached to AN^+ to form $[AN(NH_3)_n]^+$ ($n = 1$ or 2), the response of the cluster cations to the intense laser fields was found to be largely different from AN^+ [8]. The $C_5H_6^+$ yield from $[AN(NH_3)]^+$ and $[AN(NH_3)_2]^+$ are much smaller than that from the bare AN^+, indicating that the cluster formation suppresses largely the decomposition of AN^+. As shown in Fig. 3(a) and (b),
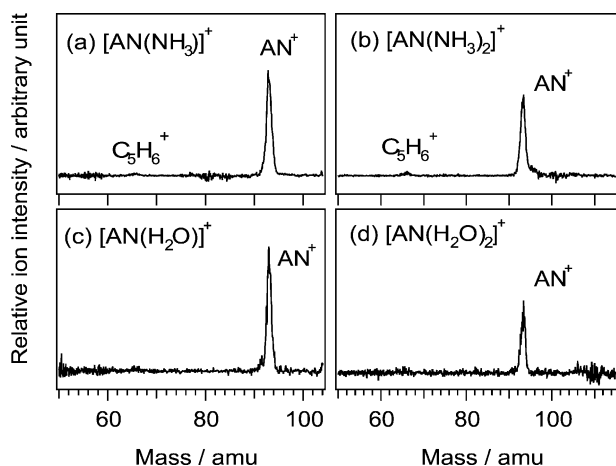
AN^+ is dominantly produced from the mass-selected parent cluster cations, $[AN(NH_3)_n]^+$ ($n = 1$, 2), and the ratios between the yields of $C_5H_6^+$ and AN^+ were 4:96 and 6:94 for $n = 1$ and 2, respectively. The yield ratios of $C_5H_6^+$ from the $[AN(NH_3)_n]^+$ ($n = 1$, 2) cluster ions with respect to the yield of the parent ions are $0.56(18) \times 10^{-3}$ and $2.2(2) \times 10^{-3}$, respectively, which are only 11 and 44% of the corresponding ratio, $5.2(3) \times 10^{-3}$, for the bare AN^+ ion.

On the other hand, as shown in Fig. 3(c) and (d), when one or two H_2O molecules are attached to AN^+, the decomposition product of $C_5H_6^+$ is not identified with detectable signal intensities. This result shows that the cluster formation with H_2O suppresses the AN^+ decomposition more efficiently than that with NH_3. On the basis of these signal-to-noise ratios of the mass spectra, the upper limits of the yield ratios of $C_5H_6^+$ from the $[AN(H_2O)_n]^+$ ($n = 1$, 2) cluster ions with respect to these parent ions are estimated to be 0.1×10^{-3} and 0.2×10^{-3}, respectively. The yield ratios for the $C_5H_6^+$ production from AN^+, $[AN(NH_3)_n]^+$ and $[AN(H_2O)_n]^+$ ($n = 1$, 2) are compared in Fig. 4.

3.2. Suppression of decomposition of AN^+ by cluster formation

Because both NH_3 and H_2O are polar molecules, having positive proton affinities of 8.84 and 7.16 eV, respectively [12], they are expected to attach to the amino group of AN^+ through hydrogen bonding stabilized by ion-dipole type attractive interaction. Previously, ab initio MO calculations and infrared vibrational spectroscopy were performed to estimate the equilibrium geometrical structures of $[AN(NH_3)]^+$ [13,14], $[AN(H_2O)]^+$ [15,16], and $[AN(H_2O)_2]^+$ [16–18]. These theoretical calculations showed that both hydrogen atoms in the amino group of

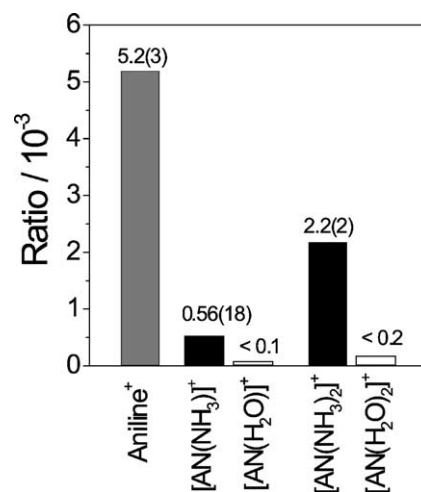Fig. 3. The mass spectra obtained when the size-selected $[AN(NH_3)_n]^+$ [8] and $[AN(H_2O)_n]^+$ ($n = 1$, 2) cluster cations are irradiated with the intense fs laser pulses ($\lambda \sim 395$ nm, $I \sim 5 \times 10^{15}$ W/cm^2). The formation of AN^+ is a dominant process for all the cluster cations. The weak signals of $C_5H_6^+$ are identified only for $[AN(NH_3)_n]^+$ ($n = 1$, 2).

Fig. 4. The relative yields of $C_5H_6^+$ with respect to the mass-selected parent cations, AN^+, $[AN(NH_3)_n]^+$ and $[AN(H_2O)_n]^+$ ($n = 1$, 2). The yields are defined by the area of the corresponding peak in the TOF spectra. The relative yields for the $[AN(H_2O)_n]^+$ ($n = 1$, 2) cluster cations are those estimated as their upper limit values on the basis of the signal-to-noise ratio of the TOF spectra.
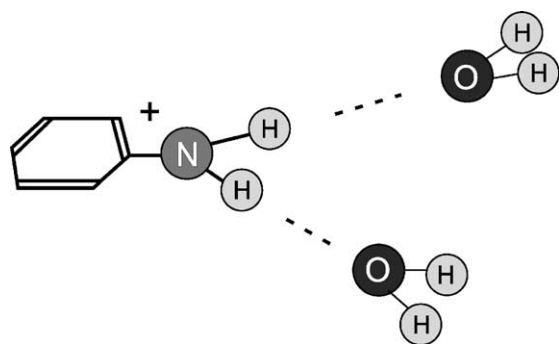
Fig. 5. The schematic diagram of the geometrical structure of $[AN(H_2O)_2]^+$.

AN^+ preferably bound to the N atom of NH_3 or the O atom of H_2O. For example, $[AN(H_2O)_2]^+$ is expected to form the geometrical structure shown in Fig. 5. The decomposition of the planar AN^+ into $C_5H_6^+$ and HNC is expected to proceed through the transition state in which the geometrical structure around the amino group is substantially deformed, since one of the two H atoms in the amino group needs to migrate into the *ortho*-carbon site by simultaneously carrying a positive charge. The observed suppression of AN^+ decomposition in $[AN(NH_3)_n]^+$ and $[AN(H_2O)_n]^+$ ($n = 1$, 2) in the intense fs laser fields indicates that the attachment of either NH_3 or H_2O to the H atom of the amino group hinders largely the migration of the hydrogen atom in the amino group by the hydrogen bond formation.

It is interesting to note that the extent of the suppression of the decomposition is larger for $[AN(H_2O)_n]^+$ than for $[AN(NH_3)_n]^+$, which may be ascribed to the difference between the binding energy for $(AN^+) \cdots NH_3$ and that for $(AN^+) \cdots H_2O$. According to the ab initio MO calculations for the $n = 1$ cluster cations using the MP2 method with the 6-31G** basis set performed by Nakanaga et al. [13], the theoretical binding energies of AN^+ with NH_3 and H_2O were 868 and 774 meV, respectively, indicating that H_2O is bound a little bit (0.094 eV) more weakly to AN^+ than NH_3.

Considering that the AN^+ moiety needs to gain the internal energy of at least ~ 3 eV for the decomposition into $C_5H_6^+$ [19], such a small difference (~ 94 meV) in the energy required for the evaporation of NH_3 and H_2O prior to the decomposition may not be a major reason for the higher efficiency of the suppression of the decomposition by the H_2O attachment than the NH_3 attachment.

3.3. Kinetic energy release of AN^+ from $[AN(NH_3)_n]^+$, and $[AN(H_2O)_n]^+$

The observed momentum-scaled TOF (MS-TOF) spectra of AN^+ produced from $[AN(NH_3)_n]^+$ and $[AN(H_2O)_n]^+$ ($n = 1$ or 2), representing the distribution of the momentum along the TOF axis, are shown in Fig. 6. The FWHMs (Δp_{obs}) of the peaks in the MS-TOF spectra for AN^+ from $[AN(NH_3)_n]^+$ ($n = 1$, 2) are $23(1) \times 10^3$ and $25(1) \times$
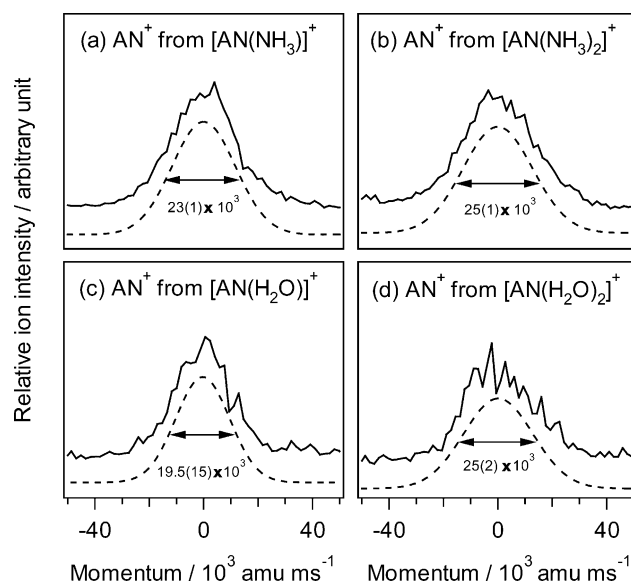

Fig. 6. The momentum-scaled TOF spectra of the AN^+ cations (solid line), which are produced from the mass-selected: (a) $[AN(NH_3)]^+$, (b) $[AN(NH_3)_2]^+$, (c) $[AN(H_2O)]^+$, and (d) $[AN(H_2O)_2]^+$ irradiated with the fs laser pulses ($\lambda \sim 395$ nm, $I \sim 5 \times 10^{15}$ W/cm^2). The dotted curves are the best-fit Gaussian distribution whose FWHM values are shown in the figures.

10^3 amu m/s, and those for AN^+ from $[AN(H_2O)_n]^+$ ($n = 1$, 2) are $19.5(15) \times 10^3$ and $25(2) \times 10^3$ amu m/s, respectively.

The FWHM values can be converted into the distribution of the momentum released through the evaporation process. By taking account of the temporal response of the tandem-type TOF measurements, 6.36(21) ns (FWHM), and by assuming that both the temporal response function expressed in a momentum scale and the momentum distribution of AN^+ have Gaussian forms, the momentum distribution of AN^+ was derived as a Gaussian function having the FWHM value (Δp) listed in Table 1. The response time of 6.36(21) ns was derived by fitting a Gaussian function to the observed peak profile of the doubly charged benzene cations photoionized from the singly charged benzene cations under the same experimental conditions.

In the case of the $n = 1$ cluster cations, the total released kinetic energies (E_{kin}) of AN^+ are converted from the HWHM ($\Delta p/2$) of the momentum distribution as listed

Table 1
The observed FWHM (Δp_{obs}) (amu m/s) of the peaks in the MS-TOF spectra for AN^+ produced from $[AN(NH_3)_n]^+$ and $[AN(H_2O)_n]^+$ ($n = 1$, 2), and the corresponding released momenta (Δp) (amu m/s) and the total kinetic energies (E_{kin}) (meV) in the evaporation processes of NH_3 and H_2O[a]

Cluster size, n	$[AN(NH_3)_n]^+$			$[AN(H_2O)_n]^+$		
	Δp_{obs}	Δp	E_{kin}	Δp_{obs}	Δp	E_{kin}
1	23(1)	22.3(10)	44.8(40)	19.5(15)	18.7(15)	30.0(52)
2	25(2)	24.4(20)	31.0(51)	25(2)	24.4(20)	29.7(25)

[a] Numbers in parentheses are estimated limits of error.

in Table 1. It can be noted that the released kinetic energy for $[AN(NH_3)]^+$ is larger than that for $[AN(H_2O)]^+$ by 14.8 meV. As described in Section 3.2, the decomposition of the AN^+ moiety into $C_5H_6^+$ proceeds more efficiently in $[AN(NH_3)]^+$ than $[AN(H_2O)]^+$ even though NH_3 is bound to AN^+ more tightly than H_2O. In addition, the released kinetic energies in the evaporation process to form AN^+ was found to be larger for $[AN(NH_3)]^+$ than for $[AN(H_2O)]^+$. These observations suggest that the internal energy of $[AN(NH_3)]^+$ gained from the laser fields is larger than that of $[AN(H_2O)]^+$. It is possible that the transition moment between the electronic ground and excited states of the AN^+ moiety is influenced by the cluster formation with NH_3 and H_2O, and that the transition moment in $[AN(NH_3)]^+$ becomes larger than that in $[AN(H_2O)]^+$, leading to the larger energy gain for $[AN(NH_3)]^+$ than for $[AN(H_2O)]^+$. It is also possible that the stabilization of $[AN(NH_3)]^+$ through the hydrogen bonding is different from $[AN(H_2O)]^+$, and that the spacing between the electronic states for $[AN(NH_3)]^+$ matches with the laser field wavelength better than that for $[AN(H_2O)]^+$. However, such a difference in the energy spacing may not become large compared with the energy spread of the short-pulsed laser fields, nor with the energy range of the entire electronic band.

In the case of the $n = 2$ cluster cations, the total released kinetic energies could not be derived a priori from the observed momentum spread, because the evaporation process is considered to be a three-body fragmentation process. However, if it is assumed that the two molecules attached to AN^+ dissociate simultaneously, and that the process can be regarded as the relative translational motion of AN^+ and a point having the mass amounting to that of these two molecules, the released kinetic energies can be calculated as listed in Table 1. It is noted that the released kinetic energies for $[AN(NH_3)_2]^+$ and $[AN(H_2O)_2]^+$ take almost the same values, and that the value for $[AN(NH_3)_2]^+$ is substantially smaller than $[AN(NH_3)]^+$. It is possible that the increase of the vibrational degrees of freedom is responsible for the smaller kinetic energy release for the $n = 2$ cluster cations. By the attachment of the second NH_3, the vibrational degrees of freedom increase, and it could result in the decrease in the energy which could be converted into the kinetic energy on the occasion of the evaporation.

4. Conclusion

When the mass-selected $[AN(H_2O)_n]^+$ ($n = 1, 2$) cations were irradiated with the intense fs laser fields ($\lambda \sim 395$ nm, $I \sim 5 \times 10^{15}$ W/cm^2, $\Delta t \sim 50$ fs), the decomposition reaction of the AN^+ moiety into $C_5H_6^+$ was not identified, and only evaporation of H_2O to form AN^+ was observed. The higher efficiency of the suppression of AN^+ decomposition by the H_2O attachment than by the NH_3 attachment was ascribed to the difference in the internal energy of the parent cluster cation gained from the intense laser fields.

It was also observed that the larger kinetic energy was released in the NH_3 evaporation from $[AN(NH_3)]^+$ than in the H_2O evaporation from $[AN(H_2O)]^+$, suggesting that the internal energy is flown into $[AN(NH_3)]^+$ more efficiently than into $[AN(H_2O)]^+$ from the intense laser fields.

The higher efficiency of the suppression of the decomposition of AN^+ by the H_2O attachment could also be interpreted as the change in the potential energy surface along the reaction coordinate for the decomposition reaction into $C_5H_6^+$. It may be possible that the barrier along the reaction coordinate, which corresponds to the motion of one of the two H atoms of the amino group, becomes larger than that for the NH_3 attachment even though the potential along the direction of the hydrogen bond becomes shallower. Further experiments such as real-time probing of the energy flow within the clusters from their energized state prepared by intense laser fields could clarify the mechanism of the suppression as well as the mechanism of the evaporation.

References

[1] K. Yamanouchi, Science 295 (2002) 1659.
[2] L.J. Frasinski, K. Codling, P. Hatherly, J. Barr, I.N. Ross, W.T. Toner, Phys. Rev. Lett. 58 (1987) 2424.
[3] B. Sheehy, L.F. DiMauro, Annu. Rev. Phys. Chem. 47 (1996) 463.
[4] P.B. Corkum, M. Yu Ivanov, J.S. Wright, Annu. Rev. Phys. Chem. 48 (1997) 387.
[5] W. Fuss, W.E. Schmid, S.A. Trushin, J. Chem. Phys. 112 (2000) 8347.
[6] R. Itakura, J. Watanabe, A. Hishikawa, K. Yamanouchi, J. Chem. Phys. 114 (2001) 5598.
[7] H. Harada, S. Shimizu, T. Yatsuhashi, S. Sakabe, Y. Izawa, N. Nakashima, Chem. Phys. Lett. 342 (2001) 563.
[8] J. Watanebe, R. Itakura, A. Hishikawa, K. Yamanouchi, J. Chem. Phys. 116 (2002) 9697.
[9] T.P. Debies, J.W. Rabalais, J. Electron Spectrosc. Relat. Phenom. 1 (1973) 355.
[10] T. Kobayashi, S. Nagakura, Bull. Chem. Soc. Jpn. 47 (1974) 2563.
[11] T. Shida, Electronic Absorption Spectra of Radical Ions, Elsevier, Amsterdam, 1988.
[12] E.P.L. Hunter, S.G. Lias, J. Phys. Chem. Ref. Data 27 (1998) 413.
[13] T. Nakanaga, K. Sugawara, K. Kawamata, F. Ito, Chem. Phys. Lett. 267 (1997) 491.
[14] Y. Inokuchi, K. Ohashi, Y. Honkawa, H. Sekiya, N. Nishi, Chem. Phys. Lett. 359 (2002) 283.
[15] T. Nakanaga, K. Kawamata, F. Ito, Chem. Phys. Lett. 279 (1997) 309.
[16] Y. Honkawa, Y. Inokuchi, K. Ohashi, N. Nishi, H. Sekiya, Chem. Phys. Lett. 358 (2002) 419.
[17] D.M. Chipman, J. Phys. Chem. A 104 (2000) 11816.
[18] T. Nakanaga, F. Ito, Chem. Phys. Lett. 348 (2001) 270.
[19] T. Baer, T.E. Carney, J. Chem. Phys. 76 (1982) 1304.